RSC Advances

PAPER

View Article Online
View Journal | View Issue

Cite this: *RSC Adv.*, 2014, **4**, 48796

Magnetic composite nanoparticles consisting of helical poly(*n*-hexyl isocyanate) and Fe_3O_4 prepared *via* click reaction†

Xuan Liu,[ab] Ru Cheng,[b] Jianping Deng*[a] and Youping Wu*[b]

A novel type of magnetic composite particles was constructed using helical poly(*n*-hexyl isocyanate) and Fe_3O_4. For this purpose, well-defined 4-ethynylbenzyloxy-terminal poly(*n*-hexyl isocyanate)s (PHIC–C≡Cs) were synthesized *via* coordination polymerization by using an organotitanium catalyst. The PHIC–C≡Cs were characterized by GPC, FT-IR and ^{1}H NMR techniques. UV-vis absorption spectra demonstrated that the PHIC–C≡Cs adopted dynamic helical structures in tetrahydrofuran. Azide-modified magnetic Fe_3O_4 nanoparticles (Fe_3O_4@N_3 NPs) were prepared through the reaction between 3-azidopropyltrimethoxysilane and oleic acid-coated magnetic Fe_3O_4 NPs. The obtained clickable PHIC–C≡C and Fe_3O_4@N_3 NPs were subjected to the Cu-catalyzed azide/alkyne cycloaddition for synthesizing the anticipated Fe_3O_4@PHIC composite NPs. FT-IR, TGA and TEM techniques confirmed the formation of the magnetic composite nanoparticles. UV-vis absorption spectra demonstrated that the PHIC chains coated on the magnetic Fe_3O_4 NPs adopted dynamic helical structures. XRD measurements revealed that coating PHIC chains on Fe_3O_4 nanoparticles did not change the phase properties of Fe_3O_4 nanoparticles. The Fe_3O_4@PHIC composite NPs showed a saturation magnetization of 17.8 emu g^{-1} and the expected rapid magnetic responsivity.

Received 23rd July 2014
Accepted 19th September 2014

DOI: 10.1039/c4ra07476a

www.rsc.org/advances

1. Introduction

Over the past few decades, magnetic nanoparticles (NPs) have received considerable attention because of their unique physical and chemical properties such as the responsivity to external magnetic fields and the production of heat under alternate magnetic fields.[1] Moreover, magnetic NPs exhibit extensive applications in separation,[2] catalysis[3] and drug delivery,[4] among others.[5,6] Fe_3O_4 NPs are the most widely investigated magnetic particles and can be prepared by various methods such as coprecipitation,[7] thermal decomposition of iron compounds,[8] hydrothermal method,[9] reverse-micelle[10] and hydrolysis of iron-organics.[11] However, the pristine magnetic Fe_3O_4 NPs tend to agglomerate due to anisotropic dipolar attraction, and they are also easily corroded by harsh environments.[12] In addition, the lack of efficient functional groups limits the practical applications of magnetic particles. To solve these issues, it is a good choice to prepare Fe_3O_4 magnetic composite NPs by grafting polymer layers on the surface of Fe_3O_4 NPs. There are two major methods to attach polymer chains onto magnetic Fe_3O_4 NPs, *i.e.*, "grafting to"[13] and "grafting from"[14] techniques. The covalent bonds formed between Fe_3O_4 NPs surface and polymer chains make the polymer layers robust and resistant to common environmental conditions. Many researchers have carried out elegant studies on preparing magnetic Fe_3O_4 composite particles. For example, Yang *et al.* synthesized boronic acid-functionalized magnetic composite microspheres for selective enrichment of glycoproteins.[15] Priestley *et al.* prepared Fe_3O_4 NPs that contained polydopamine and served as drug carriers and catalyst supports.[16] Yang *et al.* reported multilayer magnetic composite particles functionalized with polymer brushes, which were used as stabilizers for gold nanocolloids, and moreover enabled their recyclable catalysis.[17] However, to our knowledge, studies dealing with magnetic Fe_3O_4 composite NPs functionalized by synthetic helical polymer chains are still scarce. The magnetic Fe_3O_4 composite NPs containing such distinctive helical polymers shall possess interesting properties that cannot be observed in usual magnetic Fe_3O_4 composite NPs. Thus, the present study is focused on preparing a novel type of magnetic composite NPs based on Fe_3O_4 and helical poly(*n*-hexyl isocyanate) (PHIC).

Polyisocyanates[18–21] have recently received much attention because of their unique features such as the ability to form helical[22,23] and liquid crystalline[24] structures. Isocyanate polymers can adopt a predominant helicity when prepared by

[a]*State Key Laboratory of Chemical Resource Engineering, College of Materials Science and Engineering, Beijing University of Chemical Technology, Beijing 100029, China. E-mail: dengjp@mail.buct.edu.cn; Tel: +86-10-6443-5128*

[b]*State Key Laboratory of Organic-Inorganic Composites, Beijing University of Chemical Technology, Beijing 100029, China. E-mail: wuyp@mail.buct.edu.cn; Tel: +86-10-6444-2621*

† Electronic supplementary information (ESI) available: Synthesis of organotitanium(IV) catalyst and PHIC–C≡C. GPC elution profile of the PHIC–C≡Cs. All these materials were provided. See DOI: 10.1039/c4ra07476a

utilizing chiral initiators,[25] solvents[26] or monomers.[27] Helical polyisocyanates demonstrated the majority rule[28] and the sergeant-and-soldiers principle,[29,30] as originally discovered by Green *et al.* Because of their fascinating helical structures and appealing properties, polyisocyanates are recognized as good candidate materials for developing liquid crystals,[24,31,32] optical switches,[33] recognition devices[27] and so forth.[23,25,34–36] Novak group[37] prepared alkoxytitanium catalysts that effectively catalyzed the polymerization of isocyanates. However, no report has been dedicated to the preparation of helical polyisocyanates grafted on the surface of nanoparticles. We reason that a judicious combination of helical polyisocyanates and Fe_3O_4 NPs will undoubtedly give rise to a number of unique functional materials. Such magnetic composite particles are expected to show not only the magnetic properties derived from Fe_3O_4, but also certain attractive properties from helical polyisocyanates. Moreover, this novel type of magnetic composite particles may find significant applications as smart materials, optical materials, *etc.* Herein, we report a facile synthesis of magnetic composite NPs consisting of Fe_3O_4 and poly(*n*-hexyl isocyanate) (PHIC). The reason for using PHIC as a model of synthetic polyisocyanates is that PHIC has been well investigated in literature[18–21] and by our group.[38] By following the same strategy, a significant number of other novel composite particles can be prepared next.

2. Experimental section

2.1 Materials

Trichlorocyclopentadienyltitanium(IV) ($CpTiCl_3$), 4-ethynylbenzyl alcohol, ferrous sulfate heptahydrate ($FeSO_4 \cdot 7H_2O$), ferric chloride hexahydrate ($FeCl_3 \cdot 6H_2O$), oleic acid (OA), (3-chloropropyl)trimethoxysilane, sodium azide (NaN_3), copper bromide (CuBr, 99.0%), and *N*,*N*,*N*′*N*″,*N*″-pentamethyldiethylenetriamine (PMDETA) were purchased from Aldrich Chemical Co. and used as received. *n*-Hexyl isocyanate (HIC, 97%) was obtained from Aldrich. Before use, HIC was dried over calcium hydride overnight, distilled under vacuum, and then stored at −20 °C. Aqueous ammonia solution ($NH_3 \cdot H_2O$) (25%, w/w) and sodium chloride (NaCl) were purchased from Beijing Chemical Reagents Company and used without further purification. The solvents tetrahydrofuran (THF), dichloromethane (CH_2Cl_2), toluene, *N*,*N*-dimethylformamide (DMF) and methanol were purified by standard methods.[39]

2.2 Characterizations

^{1}H NMR spectra were recorded on a Bruker AV600 spectrometer with $CDCl_3$ as the solvent. FT-IR spectra were recorded with a Nicolet Nexus 670 infrared spectrometer (KBr tablet). Number-average molecular weights (M_n) and molecular weight distributions (PDI, M_w/M_n) of polymers were determined by GPC (Waters 515-2410 system) calibrated by using polystyrenes as the standards and THF as the eluent. UV-vis absorption spectra were recorded in THF on a Jasco 810 spectropolarimeter. Transmission electron microscopy (TEM) images were taken using a JEM-2100 (JEOL) transmission electron microscope at an accelerating voltage of 200 kV. Powder X-ray diffraction (XRD) patterns were recorded on a D/max2500 VB2+/PC X-ray diffractometer (Rigaku) using Cu Kα radiation in the 2θ range 10°–70°. Thermogravimetric analysis (TGA) was carried out with a Q50 TGA at a scanning rate of 10 °C min^{-1} in air. The magnetic properties were measured using a vibrating sample magnetometer (VSM, LakeShore 7410 VSM) at room temperature.

2.3 Synthesis

2.3.1 Synthesis of OA-coated magnetic Fe_3O_4 nanoparticles (Fe_3O_4@OA). Synthesis of organotitanium(IV) catalyst ($CpTiCl_2$–OCH_2Ph–C≡C) and the polymerization of HIC by the catalyst to form PHIC–C≡C are described in detail in ESI.† The synthesis of OA-coated magnetic Fe_3O_4 NPs (Fe_3O_4@OA) was accomplished by a method similar to a previous report.[12] The whole procedure was performed under an argon atmosphere. Briefly, in a 250 mL three-necked flask, $FeSO_4 \cdot 7H_2O$ (1.2 g) and $FeCl_3 \cdot 6H_2O$ (2.1 g) were added, and then dissolved in 50 mL of deionized water. After that, 13 mL $NH_3 \cdot H_2O$ (25%, w/w) was quickly added to the solution at room temperature. The color of the solution changed from orange to black, leading to a black precipitate. Then, under vigorous stirring, OA (0.6 mL) was added dropwise to the dispersion at 80 °C within 1 h. The as-synthesized Fe_3O_4@OA NPs could be well dispersed in water by the protection of the layers of OA.

The next step was to extract Fe_3O_4@OA NPs from water into toluene. Briefly, to a 250 mL extractor, the magnetic Fe_3O_4 NPs water dispersion (50 mL) and toluene (50 mL) were mixed. Fe_3O_4@OA NPs were transferred into toluene phase by adding NaCl (0.2 g). Magnetic Fe_3O_4 NPs showed good dispersibility in toluene because of the protection of a single layer of OA. Finally, the toluene dispersion was refluxed to remove most of the water under a nitrogen atmosphere, and the resulting Fe_3O_4@OA was diluted with toluene to 10 mg mL^{-1}.

2.3.2 Synthesis of 3-azidopropyltrimethoxysilane (APTMS). The synthesis of 3-azidopropyltrimethoxysilane (APTMS) was accomplished by a method similar to a previous report.[40,41] Briefly, 3-chloropropyltrimethoxysilane (1.7 mL), NaN_3 (1.5 g) and DMF (15 mL) were added to a 100 mL dried round-bottom flask. After the mixture was stirred at 80 °C for 24 h, the solid formed in the reaction mixture was removed by filtration. The filtrate was collected for the next reaction.

2.3.3 Synthesis of azide-modified magnetic Fe_3O_4 NPs (Fe_3O_4@N_3). The synthesis of azide-modified magnetic Fe_3O_4 NPs (Fe_3O_4@N_3) was accomplished by following a reported method.[40,41] The whole procedure was performed under an argon atmosphere. Typically, the Fe_3O_4@OA suspension in toluene (50 mL) and APTMS solution in DMF (15 mL) obtained above were added into a 250 mL three-necked flask. After mechanically stirring it at room temperature for 48 h, the Fe_3O_4@N_3 NPs were isolated and washed with DMF and THF three times, respectively, and then dried under vacuum at 60 °C for 12 h.

2.3.4 Synthesis of PHIC-modified magnetic Fe_3O_4 composite nanoparticles by click reaction (Fe_3O_4@PHIC). The synthesis of PHIC-modified magnetic Fe_3O_4 NPs (Fe_3O_4@PHIC) was accomplished by referring to a procedure reported in

literature.[40,42] The whole process was performed under an argon atmosphere. Typically, in a 100 mL three-necked flask, Fe_3O_4@N_3 (10 mg), PHIC–C≡C-1 (70 mg; Table 1, as representative) and CuBr (2.1 mg) were dispersed in THF (10 mL) by sonication to form a black suspension. PMDETA (6.1 μL) was added into the reaction mixture under mechanical stirring for 96 h at room temperature. The fabricated Fe_3O_4@PHIC NPs were isolated, washed with THF three times, and then dried under vacuum at 50 °C for 12 h.

3. Results and discussion

3.1 Synthesis of PHIC–C≡C

A schematic representation for preparing the designed magnetic composited nanoparticles is presented in Scheme 1. For the preparation of PHIC–C≡C, $CpTiCl_3$ was reacted with the terminal –OH group in 4-ethynylbenzyl alcohol to form the corresponding organotitanium(IV) catalyst. This kind of catalyst was effective for the polymerization of HIC, and thus used to synthesize clickable PHIC, as shown in Scheme 1. GPC, FT-IR and ^{1}H NMR spectroscopies were utilized to confirm the successful formation of PHIC–C≡C, as reported below.

Three PHIC–C≡Cs were designed and successfully prepared in the present study, as presented in Table 1 and Fig. S1 (GPC elution profiles of the polymers, in ESI†). The data in Table 1 show that on increasing the monomer/catalyst molar ratio, there was an increase in the actual molecular weights of the PHIC–C≡Cs. However, the measured molecular weights are much larger than the corresponding theoretical values. This could be explained as follows. Polyisocyanates could be regarded as rigid polymer chains. Accordingly, for the molecular weight obtained *via* GPC when calibrated by using polystyrenes as the standards, there is usually a large inflation between it and the absolute value.[42,43] Table 1 also shows that the conversion percentage of HIC is not highly satisfactory. This is due to the reversibility of the polymerization reaction of HIC with organotitanium(IV) catalysts.[37]

Fig. 1 shows the FT-IR spectra of 4-ethynylbenzyl alcohol, HIC and PHIC–C≡C-1 (taken as an example of the PHIC–C≡Cs). In the spectrum of 4-ethynylbenzyl alcohol, the broad band at 3500–3200 cm^{-1} is assigned to the –OH group, while the peaks around 2120 and 816 cm^{-1} are assigned to the alkynyl and phenyl groups, respectively. In the spectrum of HIC, the band at 2270 cm^{-1} is ascribed to the isocyanate group

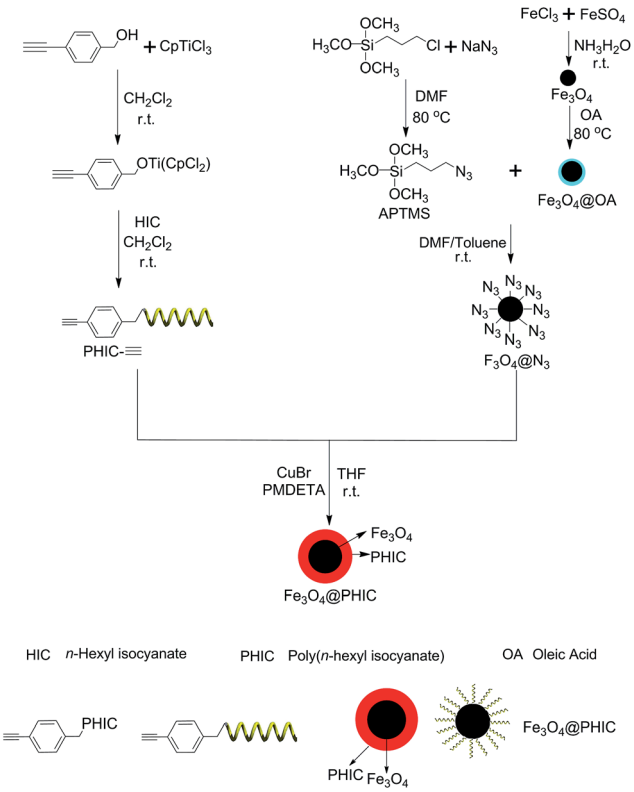

Scheme 1 A schematic representation of the synthesis of Fe_3O_4@PHIC composite nanoparticles.

stretching vibration. For the polymer PHIC–C≡C-1, the peak around 3300 cm^{-1}, which is assigned to the hydroxyl groups of 4-ethynylbenzyl alcohol, disappeared completely. In addition, the absence of absorption at 2270 cm^{-1} indicates that the obtained polymers did not contain residual isocyanate groups, *i.e.*, monomers. Nonetheless, the characteristic peak of alkynyl groups, which should appear at 2120 cm^{-1}, could hardly be observed. This is because only one alkynyl group existed at the end of each polymer chain. The characteristic peaks of –C=O and –C–N around 1715 and 1179 cm^{-1} could also be clearly observed.[38] The characteristic peak of phenyl group suffered a blue shift from 816 to 792 cm^{-1}. All the observations aforementioned demonstrate the formation of PHIC–C≡Cs.

The ^{1}H NMR spectrum of PHIC–C≡C-1 (as a model) is shown in Fig. 2. $CDCl_3$ was used as solvent for the NMR

Table 1 Parameters of the three PHIC–C≡C[a]

Run	n_{HIC}/n_{cat}[b] (mol mol^{-1})	Polymer					
		Sample code	Yield[c] (%)	DP[d]	M_n[d]	M_n[e]	PDI[d]
1	23	PHIC–C≡C-1	63.2	32	4400	3200	1.16
2	34	PHIC–C≡C-2	54.7	42	5700	4600	1.15
3	47	PHIC–C≡C-3	47.3	59	7800	6300	1.27

[a] $[HIC]_0$ = 5 mol L^{-1}; polymerization temperature, 30 °C; polymerization time, 24 h; solvent, CH_2Cl_2. [b] The monomer-to-catalyst ratio, in mole. [c] Determined gravimetrically. [d] DP, degree of polymerization; M_n, number-average molecular weight; PDI (M_w/M_n), polydispersity of molecular weight; determined by GPC in THF. [e] Determined by theoretical calculation, $M_n = (n_{HIC}/n_{cat}) \times M_{n_{HIC}} + M_{n_{catalyst}}$.

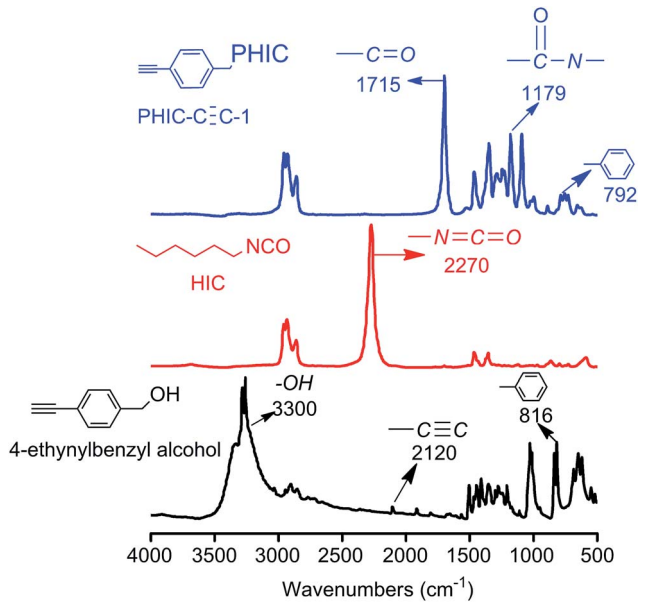

Fig. 1 FT-IR spectra for 4-ethynylbenzyl alcohol, HIC and PHIC–C≡C-1 (KBr tablet).

measurements. The peak at 2.13 ppm is assigned to the ethynyl proton in the chain end of the obtained PHIC–C≡C-1 (H_a). The signals located at chemical shifts of 7.34–7.52 ppm correspond to the phenyl protons (H_b). The peak of the methylene protons adjacent to phenyl group was observed at 5.20 ppm (H_c). The broad band at 3.77 to 3.82 ppm is assigned to the methylene protons directly attached to the N atom of HIC (H_d). The signals located at 1.65 ppm are ascribed to the methylene protons of HIC (H_e). The peak at 0.88 ppm is due to the terminal methyl protons in HIC units (H_i). The peak at 1.28 ppm indicates the other methylene protons in HIC units (H_f, H_g, H_h). As described

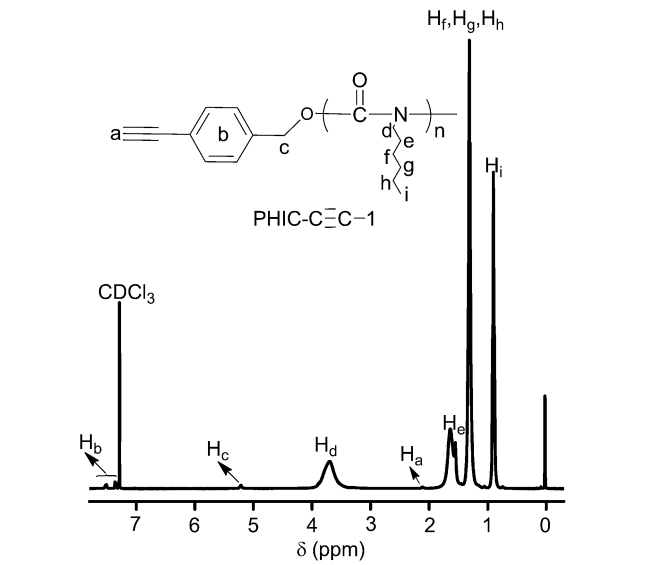

Fig. 2 Typical ^{1}H NMR spectrum of PHIC–C≡C-1 ($CDCl_3$, room temperature).

above, the characteristic resonances for all the protons of PHIC–C≡C-1 can be clearly observed at their corresponding positions, as illustrated in Fig. 2, demonstrating the successful preparation of PHIC–C≡C-1.

It is well known that polyisocyanates can form helical structures, according to the earlier studies.[23,25,34,38,44–46] UV-vis and CD spectroscopy measurements could demonstrate this conclusion. Lee *et al.*[25,34] reported that chiral PHIC macromonomers showed a positive cotton effect at 250 nm due to a characteristic n → π* transition of the polyisocyanate backbone. Therefore, the present PHIC–C≡Cs were also subjected to UV-vis absorption and CD measurements. The CD spectra showed no CD signal as expected, because no chiral center was contained in the polymers. The three PHIC–C≡Cs showed the same results, and here we consider PHIC–C≡C-1 as an example to discuss the helical structures of the PHIC–C≡Cs. Fig. 3A shows the UV-vis absorption spectra of PHIC–C≡C-1 measured in THF solution at varied temperatures. PHIC–C≡C-1 showed a strong UV-vis absorption around 250 nm. This is in good agreement with the results reported earlier by Lee *et al.*[34] and by our group.[38] Therefore, we conclude that the PHIC–C≡Cs adopted helical conformations in THF. When the temperature was altered, the UV-vis absorption intensities of PHIC–C≡C-1 showed a large difference. In detail, the UV-vis absorption decreased when temperature was increased from 20 to 60 °C. This observation demonstrates that the helical structures of PHIC–C≡Cs were dynamic helices, as introduced by Okamoto *et al.*[47]

3.2 Synthesis of Fe_3O_4@PHIC *via* click reaction

The synthesis procedure for the Fe_3O_4@PHIC composite nanoparticles is schematically illustrated in Scheme 1. There are three major steps in this synthesis procedure. Firstly, Fe_3O_4@OA NPs were prepared *via* the coprecipitation method. Secondly, the single layer of OA on the surface of magnetic Fe_3O_4 NPs was replaced by the prepared APTMS to acquire Fe_3O_4@N_3 NPs. Finally, PHIC was grafted onto magnetic Fe_3O_4 NPs *via* click reaction to prepare Fe_3O_4@PHIC composite nanoparticles. The key points in the preparation of Fe_3O_4@OA, Fe_3O_4@N_3 and Fe_3O_4@PHIC composite nanoparticles and the distinctive properties of the three microspheres are discussed below.

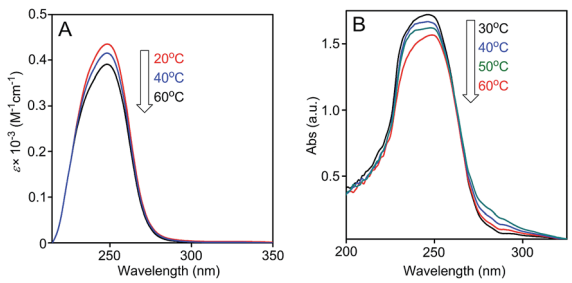

Fig. 3 UV-vis absorption spectra of PHIC–C≡C-1 (c = 0.1 mM) (A) and the Fe_3O_4@PHIC composite nanoparticles (B) measured at varied temperatures in THF.

In our research, we adopted a coprecipitation method by using OA as surfactant to acquire a stable colloidal dispersion of magnetic Fe_3O_4 NPs. By adding some salts such as NaCl, KCl, KI, or NaBr as an inducer, the magnetic Fe_3O_4 NPs were extracted into toluene.[12] APTMS was prepared from the nucleophilic substitution reaction between sodium azide and 3-chloropropyltrimethoxysilane in DMF.[41] In order to consume 3-chloropropyltrimethoxysilane completely, sodium azide was excessively loaded. Since only 3-chloropropyltrimethoxysilane and APTMS are soluble in DMF, the excessive sodium azide and the by-product could be easily removed by filtration. After that, Fe_3O_4@N_3 NPs were obtained by replacing the OA layer by APTMS. Then, PHIC was grafted onto magnetic Fe_3O_4 NPs to fabricate Fe_3O_4@PHIC composite nanoparticles using the click reaction, Cu(I)-catalyzed 1,3-dipolar cycloaddition, between the Fe_3O_4@N_3 NPs and the ethynyl-terminated PHIC.

The shape and size of the composite nanoparticles were characterized by TEM. Fig. 4 shows the typical TEM images of Fe_3O_4@OA, Fe_3O_4@N_3 and Fe_3O_4@PHIC composite nanoparticles. The Fe_3O_4@OA NPs (Fig. 4A) show either a spherical or an ellipsoidal shape with some irregularities. The particle size distribution histogram of Fe_3O_4@OA NPs calculated from the TEM images is shown in Fig. 4B. It can be clearly seen that the Fe_3O_4@OA NPs had a narrow size distribution with an average particle size of 18 ± 1 nm (after analysis of over 100 nanoparticles). The OA layer on the surface of magnetic Fe_3O_4 NPs played an important role in improving the dispersion of magnetic Fe_3O_4 NPs.[12] Fig. 4C and D show that the Fe_3O_4@N_3 NPs possessed similar shape, size and size distribution to those of the Fe_3O_4@OA NPs (after analysis of over 50 nanoparticles). However, the Fe_3O_4@N_3 NPs aggregated to some degree, because the OA layer was substituted by APTMS. The Fe_3O_4@PHIC composite nanoparticles (Fig. 4E) noticeably demonstrated a PHIC layer coated on the surface of the magnetic Fe_3O_4 NPs. Compared with the Fe_3O_4@N_3 NPs, the Fe_3O_4@PHIC composite nanoparticles aggregated more noticeably. This could be explained by the interaction force among PHIC chains. Because of the noticeable aggregation of the Fe_3O_4@PHIC composite nanoparticles, it is difficult to obtain the particle size distribution histogram of Fe_3O_4@PHIC NPs, as can be seen in the TEM images. All the observations mentioned above indicate that PHIC was successfully attached on the surface of the magnetic Fe_3O_4 NPs. This hypothesis was further confirmed by the following characterizations.

The crystal phases of magnetic products were investigated by XRD analysis. Fig. 5 displays the XRD patterns of the Fe_3O_4@N_3 NPs and Fe_3O_4@PHIC composite nanoparticles. These two sets of nanoparticles show similar diffraction peaks at $2\theta = 18.4°$, 30.1°, 35.6°, 37.2°, 43.1°, 53.5°, 57.1°, and 62.7°. These peaks correspond to the (111), (220), (311), (222), (400), (422), (511), and (400) lattice planes, respectively, which are in agreement with the literature data.[11,12] All the observed peaks in the patterns can be indexed to the face centered cubic phase of Fe_3O_4.[48] The results revealed that the chemical modification of Fe_3O_4 nanoparticles by PHIC did not change the phase properties of Fe_3O_4 nanoparticles.

All the samples of PHIC–C≡C, Fe_3O_4@N_3 and Fe_3O_4@PHIC were characterized by FT-IR spectroscopy. The relevant spectra are illustrated in Fig. 6, with PHIC–C≡C-1 as an example. The FT-IR spectrum of PHIC–C≡C-1 has been discussed above. In the spectrum of Fe_3O_4@N_3 NPs, the band at 2106 cm^{-1} is assigned to N=N=N antisymmetric stretching vibration in azide.[49] The characteristic peak of Fe–O stretching vibration can be found at 590 cm^{-1}.[50] For the Fe_3O_4@PHIC composite nanoparticles, the band at 1545 cm^{-1} is assigned to 1,2,3-

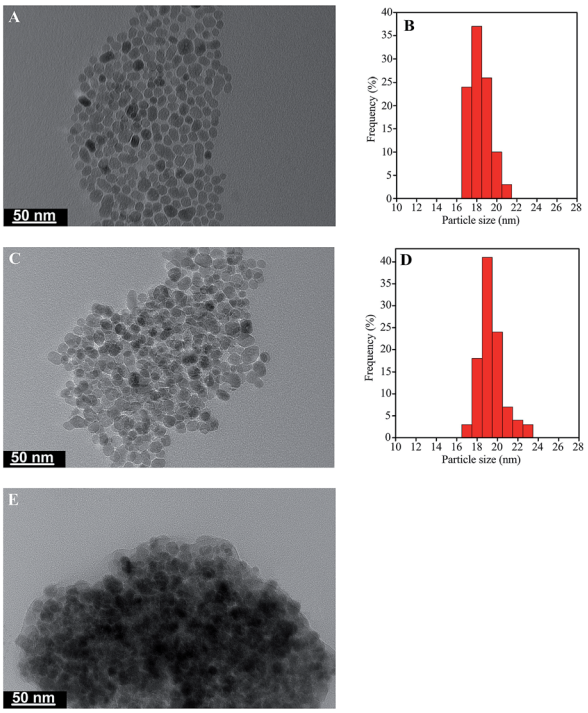

Fig. 4 TEM images of particles: (A) Fe_3O_4@OA, (C) Fe_3O_4@N_3, and (E) Fe_3O_4@PHIC. Particle size distribution histograms of Fe_3O_4@OA (B) and Fe_3O_4@N_3 (D) nanoparticles, calculated from the TEM images.

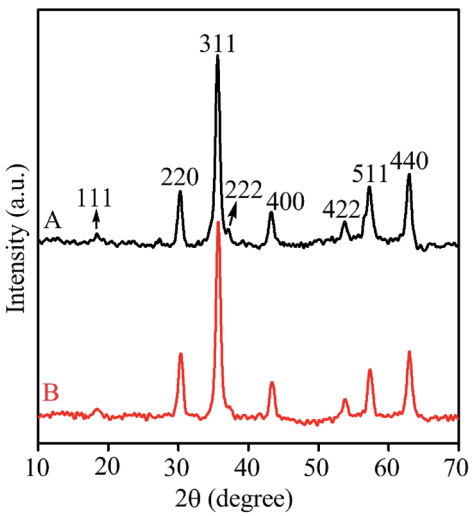

Fig. 5 XRD patterns of: (A) Fe_3O_4@N_3, and (B) Fe_3O_4@PHIC nanoparticles.

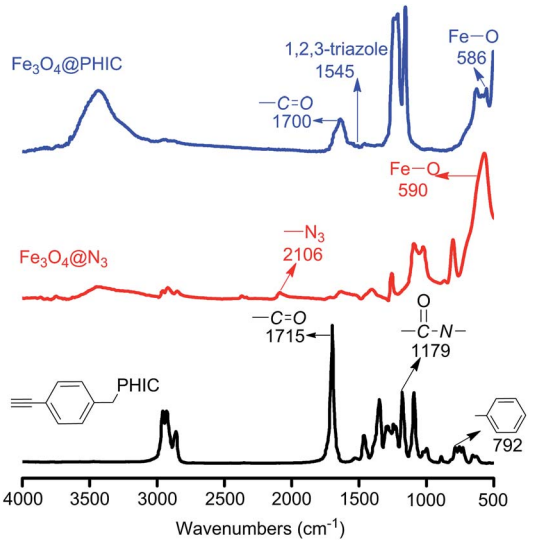

Fig. 6 FT-IR spectra for PHIC–C≡C-1, Fe_3O_4@N_3 and Fe_3O_4@PHIC (KBr tablet).

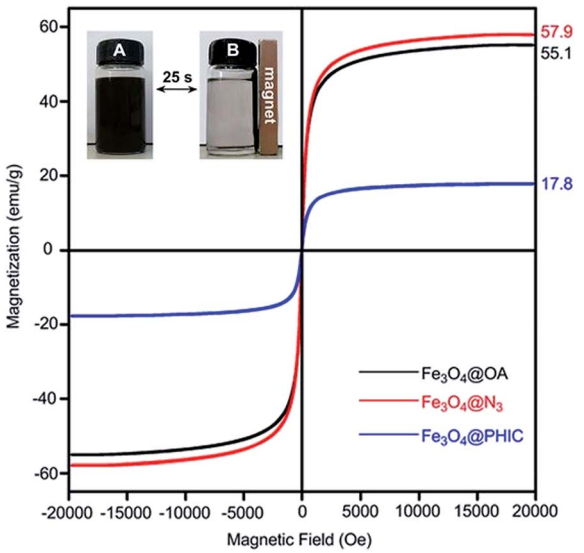

Fig. 7 VSM magnetization curves of Fe_3O_4@OA, Fe_3O_4@N_3 and Fe_3O_4@PHIC composite nanoparticles at room temperature. The inset shows the responsivity of the Fe_3O_4@PHIC composite nanoparticles when exposed to an external magnetic field. The time from state (A) to state (B) was 25 s.

triazole.[49] The bands for alkyne (2120 cm^{-1}) and azide (2106 cm^{-1}) cannot be observed in the samples, demonstrating the successful conversion of alkyne and azide groups to 1,2,3-triazole by the click reaction. Moreover, there are also bands at 1700 cm^{-1} due to the C=O stretching vibration in PHIC–C≡C and 586 cm^{-1} due to the Fe–O stretching vibration in magnetic Fe_3O_4 NPs, which clearly demonstrates that PHIC was chemically grafted on the surface of magnetic Fe_3O_4 NPs through the click reaction.

As discussed in the synthesis of PHIC–C≡Cs, we have demonstrated that UV-vis absorption spectroscopy is an effective means for identifying the helical structures of PHIC. The above-obtained Fe_3O_4@PHIC composite nanoparticles were also subjected to UV-vis spectroscopy measurements. Unfortunately, we cannot directly and quantitatively characterize the second structures of PHICs due to the particle state. The UV-vis spectra only provided qualitative information (Fig. 3B). Herein, we point out that, as discussed above, no CD effect was observed in the CD spectra of the Fe_3O_4@PHIC composite nanoparticles. Fig. 3B shows the UV-vis spectra of the Fe_3O_4@PHIC composite nanoparticles measured in THF solution at varied temperatures. The Fe_3O_4@PHIC composite nanoparticles showed a strong UV-vis absorption around 250 nm. In addition, the UV-vis absorption decreased when the temperature was increased from 30 to 60 °C. These results demonstrated the existence of dynamic helical structures in the PHIC chains forming the composite nanoparticles.

Magnetic properties are necessary for practical applications of magnetic materials. Field dependent magnetization measurements on the samples were conducted to study the magnetic behaviors. Fig. 7 shows the VSM magnetization curves of Fe_3O_4@OA, Fe_3O_4@N_3 and Fe_3O_4@PHIC composite nanoparticles measured at room temperature. No obvious magnetic hysteresis loop was observed for any of the three samples. In other words, the remanence did not exist when the magnetic field was removed, indicating that all the particles possessed superparamagnetic features originating from the magnetite inner cores. The maximum saturation magnetization (MSM) of Fe_3O_4@OA, Fe_3O_4@N_3 and Fe_3O_4@PHIC composite nanoparticles was 55.1, 57.9 and 17.8 emu g^{-1}, respectively. The MSM of Fe_3O_4@OA was lower than that of Fe_3O_4@N_3, since the content of OA was higher than that of APTMS. This was also observed from the TGA analysis, as discussed next. In addition, with the coating of the non-magnetic PHIC layers onto the magnetic Fe_3O_4 NPs, the MSM of the resulting Fe_3O_4@PHIC composite nanoparticles was remarkably reduced due to the decrease in the mass content of the magnetite component. The inset in Fig. 7 shows that the Fe_3O_4@PHIC composite nanoparticles dispersion in THF responded quickly to an external magnet. The time from state (A) to state (B) was within 25 s. When the external magnet was taken off, the aggregated particles could be re-dispersed in a solvent just by shaking. This quick responsivity of Fe_3O_4@PHIC composite nanoparticles is extremely important for practical applications, particularly in terms of recycling.

The thermal stability and the composition of the composite nanoparticles were explored by thermogravimetric analysis. Fig. 8 shows the TGA curves of Fe_3O_4@OA, Fe_3O_4@N_3 and Fe_3O_4@PHIC nanoparticles. The weight loss in the Fe_3O_4@OA and the Fe_3O_4@N_3 was 14.7% and 12.5%, respectively. Both the two kinds of nanoparticles exhibited a two-stage weight-loss process. The first loss until 255 °C was due to the evaporation of physically absorbed water or solvent, and the second major weight loss from 255 to 450 °C was due to the decomposition of the low molecular organics attached on the surface of magnetic Fe_3O_4 NPs (OA for Fe_3O_4@OA and APTMS for Fe_3O_4@N_3). In addition, the weight loss in the Fe_3O_4@OA NPs was slightly

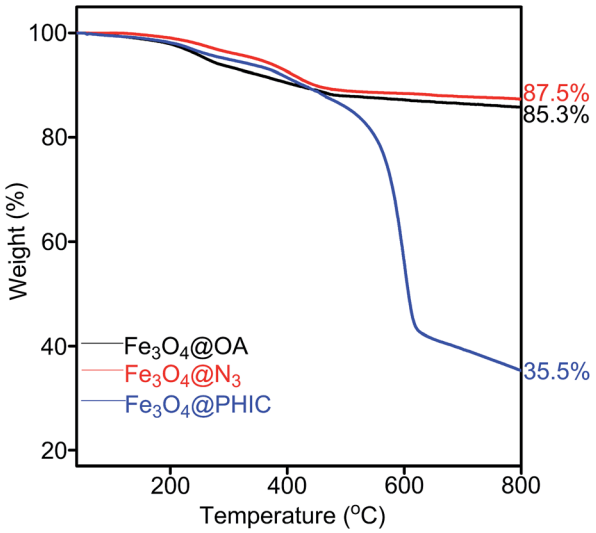

Fig. 8 TGA curves of Fe_3O_4@OA, Fe_3O_4@N_3 and Fe_3O_4@PHIC. The measurements were performed in air.

higher than that in the Fe_3O_4@N_3 NPs. This is because the content of OA was higher than that of APTMS, similar to the observation in VSM (Fig. 7). The Fe_3O_4@PHIC composite nanoparticles also decomposed in two stages. The first weight loss (about 5.2 wt%) till 250 °C was also due to the evaporation of physically absorbed water or solvent. About 59.3 wt% loss of weight occurred when temperature rose from 250 to 800 °C. During this stage, the PHIC component in the Fe_3O_4@PHIC composite nanoparticles disintegrated gradually. The TGA curve of the Fe_3O_4@PHIC composite nanoparticles exhibited a remarkably higher weight loss relative to the Fe_3O_4@N_3 nanoparticles, which further demonstrated that PHIC was efficiently coated on the magnetic Fe_3O_4 NPs *via* click reaction.

4. Conclusions

In this study, the synthesis of well-defined PHIC–C≡Cs was achieved *via* coordination polymerization by using organotitanium catalysts. The formation and the structures of the PHIC–C≡Cs were systemically confirmed by GPC, FT-IR and ^{1}H NMR measurements. UV-vis spectra demonstrated the dynamic helical structures of the PHIC–C≡Cs. The reaction between APTMS and Fe_3O_4@OA NPs resulted in Fe_3O_4@N_3 NPs. Fe_3O_4@PHIC composite nanoparticles were prepared through the Cu-catalyzed azide/alkyne cycloaddition between PHIC–C≡Cs and Fe_3O_4@N_3 NPs. The magnetic composite nanoparticles were characterized by FT-IR, XRD, TGA and TEM techniques. UV-vis spectra demonstrated that the PHIC chains coated on the magnetic Fe_3O_4 nanoparticles still formed dynamic helical structures, as in the solution state. According to VSM measurements, Fe_3O_4@PHIC composite nanoparticles exhibited a magnetization of 17.8 emu g^{-1}. The magnetic Fe_3O_4@PHIC composite nanoparticles could be separated quickly by an external magnetic field.

Acknowledgements

The project was supported by the "National Natural Science Foundation of China" (21474007, 21274008, 21174010) and the "Specialized Research Fund for the Doctoral Program of Higher Education" (SRFDP 20120010130002).

Notes and references

1 S. Laurent, D. Forge, M. Port, A. Roch, C. Robic, L. V. Elst and R. N. Muller, *Chem. Rev.*, 2008, **108**, 2064.
2 H. W. Gu, P.-L. Ho, K. W. T. Tsang, L. Wang and B. Xu, *J. Am. Chem. Soc.*, 2003, **125**, 15702.
3 J. P. Ge, Q. Zhang, T. R. Zhang and Y. D. Yin, *Angew. Chem., Int. Ed.*, 2008, **47**, 8924.
4 J. Kim, H. S. Kim, N. Lee, T. Kim, H. Kim, T. Yu, I. C. Song, W. K. Moon and T. Hyeon, *Angew. Chem., Int. Ed.*, 2008, **47**, 8438.
5 T.-J. Yoon, J. S. Kim, B. G. Kim, K. N. Yu, M.-H. Cho and J.-K. Lee, *Angew. Chem., Int. Ed.*, 2005, **44**, 1068.
6 Y.-W. Jun, Y.-M. Huh, J.-S. Choi, J.-H. Lee, H.-T. Song, S. Kim, S. Yoon, K.-S. Kim, J.-S. Shin, J.-S. Suh and J. Cheon, *J. Am. Chem. Soc.*, 2005, **127**, 5732.
7 Z. Li, B. Tan, M. Allix and A. I. Cooper, *Small*, 2008, **4**, 231.
8 S. H. Sun and H. Zeng, *J. Am. Chem. Soc.*, 2002, **124**, 8204.
9 A. Cabañas and M. Poliakoff, *J. Mater. Chem.*, 2001, **11**, 1408.
10 J. Lee, Y. Lee, J. K. Youn, H. B. Na, T. Yu, H. Kim, S.-M. Lee, Y.-M. Koo, J. H. Kwak, H. G. Park, H. N. Chang, M. Hwang, J.-G. Park, J. Kim and T. Hyeon, *Small*, 2008, **4**, 143.
11 K. Hayashi, M. Moriya, W. Sakamoto and T. Yogo, *Chem. Mater.*, 2009, **21**, 1318.
12 Y. B. Sun, X. B. Ding, Z. H. Zheng, X. Cheng, X. H. Hu and Y. X. Peng, *Eur. Polym. J.*, 2007, **43**, 762.
13 M.-Q. Zhu, L.-Q. Wang, G. J. Exarhos and A. D. Q. Li, *J. Am. Chem. Soc.*, 2004, **126**, 2656.
14 T. Wu, Y. F. Zhang, X. F. Wang and S. Y. Liu, *Chem. Mater.*, 2008, **20**, 101.
15 M. R. Pan, Y. F. Sun, J. Zheng and W. L. Yang, *ACS Appl. Mater. Interfaces*, 2013, **5**, 8351.
16 R. Liu, Y. L. Guo, G. Odusote, F. L. Qu and R. D. Priestley, *ACS Appl. Mater. Interfaces*, 2013, **5**, 9167.
17 B. Liu, D. W. Zhang, J. C. Wang, C. Chen, X. L. Yang and C. X. Li, *J. Phys. Chem. C*, 2013, **117**, 6363.
18 P. N. Shah, J. Min, C.-G. Chae, N. Nishikawa, D. Suemasa, T. Kakuchi, T. Satoh and J.-S. Lee, *Macromolecules*, 2012, **45**, 8961.
19 S. Mayer and R. Zentel, *Prog. Polym. Sci.*, 2001, **26**, 1973.
20 M. Kikuchi, L. T. N. Lien, A. Narumi, Y. Jinbo, Y. Izumi, K. Nagai and S. Kawaguchi, *Macromolecules*, 2008, **41**, 6564.
21 J. Min, P. N. Shah, J.-H. Ahn and J.-S. Lee, *Macromolecules*, 2011, **44**, 3211.
22 Y.-D. Shin, J.-H. Ahn and J.-S. Lee, *Macromol. Rapid Commun.*, 2001, **22**, 1041.
23 P. N. Shah, J. Min and J.-S. Lee, *Chem. Commun.*, 2012, **48**, 826.
24 K.-L. Tse and A. D. Shine, *Macromolecules*, 2000, **33**, 3134.

25 G. Y. Nath, S. Samal, S.-Y. Park, C. N. Murthy and J.-S. Lee, *Macromolecules*, 2006, **39**, 5965.
26 C. A. Khatri, Y. Pavlova, M. M. Green and H. Morawetz, *J. Am. Chem. Soc.*, 1997, **119**, 6991.
27 K. Maeda and Y. Okamoto, *Macromolecules*, 1998, **31**, 1046.
28 M. M. Green, B. A. Garetz, B. Munoz, H. P. Chang, S. Hoke and R. G. Cooks, *J. Am. Chem. Soc.*, 1995, **117**, 4181.
29 M. M. Green, N. C. Peterson, T. Sato, A. Teramoto, R. Cook and S. Lifson, *Science*, 1995, **268**, 1860.
30 S. k. Jha, K.-S. Cheon, M. M. Green and J. V. Selinger, *J. Am. Chem. Soc.*, 1999, **121**, 1665.
31 J.-H. Kim, M. S. Rahman, J.-S. Lee and J.-W. Park, *J. Am. Chem. Soc.*, 2007, **129**, 7756.
32 J.-H. Kim, M. S. Rahman, J.-S. Lee and J.-W. Park, *Macromolecules*, 2008, **41**, 3181.
33 D. Pijper, M. G. M. Jongejan, A. Meetsma and B. L. Feringa, *J. Am. Chem. Soc.*, 2008, **130**, 4541.
34 P. N. Shah, J. Min, H.-J. Kim, S.-Y. Park and J.-S. Lee, *Macromolecules*, 2011, **44**, 7917.
35 Y.-D. Shin, J.-H. Ahn and J.-S. Lee, *Polymer*, 2001, **42**, 7979.
36 G. Maxein, S. Mayer and R. Zentel, *Macromolecules*, 1999, **32**, 5747.
37 T. E. Patten and B. M. Novak, *J. Am. Chem. Soc.*, 1996, **118**, 1906.
38 X. Liu, J. P. Deng, Y. P. Wu and L. Q. Zhang, *Polymer*, 2012, **53**, 5717.
39 D. Uhrig and J. W. Mays, *J. Polym. Sci., Part A: Polym. Chem.*, 2005, **43**, 6179.
40 J. C. Chen, M. Z. Liu, C. Chen, H. H. Gong and C. M. Gao, *ACS Appl. Mater. Interfaces*, 2011, **3**, 3215.
41 D. L. Meng, J. H. Sun, S. D. Jiang, Y. Zeng, Y. Li, S. K. Yan, J. X. Geng and Y. Huang, *J. Mater. Chem.*, 2012, **22**, 21583.
42 T. Satoh, R. Ihara, D. Kawato, N. Nishikawa, D. Suemasa, Y. Kondo, K. Fuchise, R. Sakai and T. Kakuchi, *Macromolecules*, 2012, **45**, 3677.
43 S. H. Goodson and B. M. Novak, *Macromolecules*, 2001, **34**, 3849.
44 H. Gu, Y. Nakamura, T. Sato, A. Teramoto, M. M. Green and C. Andreola, *Polymer*, 1999, **40**, 849.
45 J. Wu, E. M. Pearce, T. K. Kwei, A. A. Lefebvre and N. P. Balsara, *Macromolecules*, 2002, **35**, 1791.
46 M. M. Green, J. W. Park, T. Sato, A. Teramoto, S. Lifson, R. L. B. Selinger and J. V. Selinger, *Angew. Chem., Int. Ed.*, 1999, **38**, 3138.
47 T. Nakano and Y. Okamoto, *Chem. Rev.*, 2001, **101**, 4013.
48 A. Dong, S. Lan, J. F. Huang, T. Wang, T. Y. Zhao, L. H. Xiao, W. W. Wang, X. Zheng, F. Q. Liu, G. Gao and Y. X. Chen, *ACS Appl. Mater. Interfaces*, 2011, **3**, 4228.
49 K. Hayashi, K. Ono, H. Suzuki, M. Sawada, M. Moriya, W. Sakamoto and T. Yogo, *ACS Appl. Mater. Interfaces*, 2010, **2**, 1903.
50 D. Liu, H. Y. Chen, J. P. Deng and W. T. Yang, *J. Mater. Chem. C*, 2013, **1**, 8066.